

Kalman Filter Face-Off

Extended vs. Unscented Kalman Filters for Integrated GPS and MEMS Inertial



Copyright iStock.com/Peeter Viisimaa

GPS and micro-electro-mechanical (MEMS) inertial systems have complementary qualities that make integrated navigation systems more robust. GPS maintains good accuracy but is subject to signal blockages; low-cost MEMS are unaffected by satellite signal outages but their accuracy degrades rapidly over time. Kalman filter techniques can help bring these two technologies together synergistically. But which Kalman filtering design works best? A group of Canadian researchers tackles the question.

NASER EL-SHEIMY, EUN-HWAN SHIN, XIAO JIN LIU
MOBILE MULTI-SENSORS SYSTEMS RESEARCH
GROUP, DEPARTMENT OF GEOMATICS ENGINEERING,
THE UNIVERSITY OF CALGARY, CANADA

Today, most vehicle navigation systems rely mainly on Global Positioning System (GPS) receivers as the primary source of information to provide the vehicle position for an unlimited number of users anywhere on the planet. Since its advent, the number of applications using GPS has increased dramatically and include tracking the location and speed of people, truck fleets, trains, ships, or planes; directing emergency vehicles to the scene of an accident; mapping where a city's assets are located; and providing precise timing for endeavors that require large-scale co-ordination.

GPS, however, can reliably provide

these types of information only under ideal conditions, that is, in open areas in which GPS satellite signals can be received. In other words, the system doesn't work very well in urban canyons, canopy areas, and similar environments due to signal blockage and attenuation deteriorating the obtainable positioning accuracy. For the moment, any sophisticated urban application that demands essentially continuous position determination, cannot depend on GPS as a stand-alone system — those who have tried are still trying!

Cost and space constraints are currently driving manufacturers of vehicles to investigate and develop the next generation of low-cost and small-size navigation and guidance systems to meet the fast growing demand for in the location-based services and telematics markets. Advances in micro-

electro-mechanical systems (MEMS) technology have shed promising light on the development of such systems. But such sensors high noise and drift rate remain a problem, which may be alleviated in combination with GPS. Solutions that integrate navigation data have been recognized as the most challenging aspects that remain to turn MEMS-based inertial systems into robust, accurate navigation systems.

Introducing MEMS

The last two decades have shown an increasing demand for low-cost and miniature inertial sensors for many navigation applications. MEMS-based inertial sensors efficiently meet this demand. However, due to their lightweight and fabrication process, MEMS sensors still have some performance limitations, which consequently affect their obtainable accuracy and sensitivity.

One of the main problems of MEMS sensors is that the remaining uncertainties of the sensor errors (bias, scale factor, and noise) are very large and sensitive to surrounding environmental changes. Therefore, navigation algorithms (i.e., estimators) should be able to deal with these uncertainties.

Traditionally the linearized Kalman filter (LKF) or the extended Kalman filter (EKF) have been used in the area of navigation, and recently the unscented Kalman filter (UKF) has been proposed for low-cost inertial navigation. The UKF approach offers several benefits. Because we do not need to develop a space navigator error model for a UKF, the system development time can be reduced. Moreover, because UKF is a second order filter, higher-order errors neglected by the EKF can be considered.

As discussed in the paper by Naser El-Sheimy and Eun-Hwan Shin (2004) cited in the Additional Resources section at the end of this article, a UKF can handle large attitude errors. Hence, we can use the UKF in navigation systems based on crude inertial measurement units (IMUs)

In this article, we will compare the EKF with the UKF in terms of the state model equations and structure of the filters. Then we compare the performance of both filters by testing integrated GPS and MEMS-based IMU

systems in land vehicle environments.

The testing process includes three MEMS-based IMUs. The first two IMUs are currently available in the market, while the third one is a custom-built IMU developed by the Mobile Multi-Sensor Systems Research Group at the University of Calgary. The custom-built IMU integrates three accelerometers and three gyroscopes. In this article, we pay special attention to the filters' performance during the in-motion alignment and to the obtained positioning errors during GPS outages.

We begin by reviewing implementation of the EKF and the UKF for the integration of low-cost INS (see Table 1 for a comparison of the performance and cost of different INS grades) and GPS. Next, we will compare the performance of the two filters using three different MEMS-based IMUs and then draw conclusions from the test results.

A Profile: the EKF

Traditionally, error state Kalman filters — either the LKF or the EKF — were used in the field of navigation. If an INS error control loop (feedback) exists, then the LKF can be considered as the EKF. A low-cost INS cannot operate for a long time without the feedback loop. Hence, this article will only discuss EKF implementation.

In developing the EKF, the system

process model and the measurement model have to be linearized. In an aided inertial navigation system, the system process model comprises the INS mechanization, a description of the evolution of the navigation parameters (position, velocity and attitude), and the inertial sensor error models. Linearization of the system model can be done through perturbation analysis, a classical approach to INS error analysis. In the perturbation analysis, the navigation parameters are perturbed with respect to the true navigation frame (n-frame).

Alternatively, we can also analyze the INS error with respect to the computer frame (c-frame), the frame that the INS computer assumes to be the true navigation frame. The choice of an appropriate INS error model depends upon the given navigation scenario and is an important part of the navigation software design.

Regardless of the choice of the INS error model, the linearized system model can be described in discrete time as

$$\delta \mathbf{x}_{k+1} = \Phi_k \delta \mathbf{x}_k + \mathbf{w}_k \quad (1)$$

where $\delta \mathbf{x}_k$ is the error state vector at time t_k , Φ_k is the state transition matrix, and \mathbf{w}_k is the driven response at t_{k+1} due to the presence of the input white noise during the time interval. Because a white sequence is a sequence of a zero-mean random variable that is uncorrelated time-wise, the covariance matrix associated with \mathbf{w}_k is given as

$$E \left[\mathbf{w}_k \mathbf{w}_i^T \right] = \begin{cases} \mathbf{Q}_k, & i = k \\ 0, & i \neq k \end{cases} \quad (2)$$

The linearized measurement equation can be written as follows:

$$\delta \mathbf{z}_k = \mathbf{H}_k \delta \mathbf{x}_k + \mathbf{e}_k \quad (3)$$

where $\delta \mathbf{z}_k$ is the measurement vector; \mathbf{H}_k is a design matrix; and \mathbf{e}_k is the measurement noise vector. The measurement covariance matrix is written as

Grade	Navigation	Tactical	Automotive	Consumer
Position Error	1.9 (km/hr)	19 – 38 (km/hr)	≈2(km/min)	≈3-5(km/min)
Gyros				
Bias (deg/hr)	0.005 – 0.01	1-10	≈ 180	360 - 3600
Scalefactor(ppm)	5 -50	200 -500		
Noise(deg/hr/√Hz)	0.002–0.005	0.2 – 0.5		
Accel				
Bias (mg)	5 -10	200 – 500	≈ 1200	≈ 2400
Scalefactor(ppm)	10 – 20	400 – 1000		
Noise(mg/hr/√Hz)	5 – 10	200 - 400		
Price (US\$)	≈ 100K	10K – 60K	1K – 5K	100 – 300
Mass Production	No	No	Yes	Yes

TABLE 1. Comparison of Different INS Grades

$$E[\mathbf{e}_k \mathbf{e}_i^T] = \begin{cases} \mathbf{R}_k, & i = k \\ 0, & i \neq k \end{cases} \quad (4)$$

The system noise \mathbf{w}_k and measurement noise \mathbf{e}_k are assumed to be uncorrelated, i.e. $E[\mathbf{w}_k \mathbf{e}_i^T] = 0$ for all i, k .

Another Profile: the UKF

In the UKF, system noises are generated and are passed through the system process model. So, the state vector, \mathbf{x} , and the system noise vector, \mathbf{w} , are augmented to create the augmented state vector, \mathbf{x}^a :

$$\mathbf{x}^a = \begin{bmatrix} \mathbf{x} \\ \mathbf{w} \end{bmatrix} \quad (5)$$

The UKF is based on transforming a set of deterministically chosen points, called the sigma points, through the nonlinear system process and measurement models. The unscented transformation (UT) refers to the procedure of obtaining a set of the sigma points (SPs), χ_i^a , and the associated weights, w_i , from the given mean, $\hat{\mathbf{x}}^a$, and covariance, \mathbf{P}^a , satisfying

$$\begin{cases} \sum_{i=0}^{p-1} w_i = 1 \\ \sum_{i=0}^{p-1} w_i \chi_i^a = \hat{\mathbf{x}}^a \\ \sum_{i=0}^{p-1} w_i (\chi_i^a - \hat{\mathbf{x}}^a)(\chi_i^a - \hat{\mathbf{x}}^a)^T = \mathbf{P}^a \end{cases} \quad (6)$$

where p is the number of sigma points. Of several proposals for the UT, the scaled spherical simplex UT was applied in this paper because it generates minimal number of SPs. Scaling the sigma points is an important step in attitude estimation.

The UKF is a straightforward extension of the UT to the recursive estimation. First, we initialize the augmented states and covariance as follows:

$$\hat{\mathbf{x}}_0^a = \begin{bmatrix} \hat{\mathbf{x}}_0 \\ 0 \end{bmatrix}, \mathbf{P}_0^a = \begin{bmatrix} \mathbf{P}_0 & 0 \\ 0 & \mathbf{Q} \end{bmatrix}, \quad (7)$$

where

$$\mathbf{P}_0 = E[(\mathbf{x}_0 - \hat{\mathbf{x}}_0)(\mathbf{x}_0 - \hat{\mathbf{x}}_0)^T]$$

and $\mathbf{Q} = E[\mathbf{w}\mathbf{w}^T]$.

Then, the scaled simplex SPs are generated. During the prediction stage, the SPs go through the nonlinear system process model

$$\chi_{i,k}^{\prime-} = m\left[t_k, \chi_{i,k-1}^{a+}, \omega_{ib}^b(t_k), \mathbf{f}^b(t_k)\right] \quad (8)$$

where the superscript ‘+’ and ‘-’ denote the updated and predicted states, respectively; ω_{ib}^b is the rotation rate of the body frame with respect to the inertial frame; and \mathbf{f}^b is the specific force measurement. (The article by Shin (2004) cited in the Additional Resources section describes the system process model $m[\cdot]$ well.) Then, the predicted mean and covariance are computed using the transformed sigma points as follows:

$$\hat{\mathbf{x}}_k^- = \sum_{i=0}^{p-1} w_i^m \chi_{i,k}^{\prime-} \quad (9)$$

$$\mathbf{P}_k^- = \sum_{i=0}^{p-1} w_i^c [\chi_{i,k}^{\prime-} - \hat{\mathbf{x}}_k^-][\chi_{i,k}^{\prime-} - \hat{\mathbf{x}}_k^-]^T \quad (10)$$

where w_i^m and w_i^c are weights for the mean and covariance computation, respectively.

During the update state, the sigma points are transformed through the measurement model:

$$\mathbf{z}_{i,k}^- = h[\chi_{i,k}^{\prime-}] \quad (11)$$

The predicted measurement is computed as:

$$\hat{\mathbf{z}}_k^- = \sum_{i=0}^{p-1} w_i^m \mathbf{z}_{i,k}^- \quad (12)$$

Then, the rest of the update equations can be written as follows:

$$\Delta \mathbf{z}_{i,k}^- = \mathbf{z}_{i,k}^- - \hat{\mathbf{z}}_k^- \quad (13)$$

Unscented Kalman filters have a number of clear advantages.

The mean and covariance of the state estimate is calculated to second order or better, as opposed to first order in the EKF. This leads to a more accurate implementation of the optimal recursive estimation equations, which is the basis for both the EKF and UKF.

No explicit Jacobian or Hessian calculations are necessary for the UKF. This is especially valuable in situations where the system is a “black box” model in which the internal dynamic equations are unavailable.

$$\mathbf{P}_{vv} = \sum_{i=0}^{p-1} w_i^c [\Delta \mathbf{z}_{i,k}^-][\Delta \mathbf{z}_{i,k}^-]^T + \mathbf{R}_k \quad (14)$$

$$\mathbf{P}_{zx} = \sum_{i=0}^{p-1} w_i^c [\chi_{i,k}^{\prime-} - \hat{\mathbf{x}}_k^-][\Delta \mathbf{z}_{i,k}^-]^T \quad (15)$$

$$\mathbf{K}_k = \mathbf{P}_{zx} \mathbf{P}_{vv}^{-1} \quad (16)$$

$$\hat{\mathbf{x}}_k^+ = \hat{\mathbf{x}}_k^- + \mathbf{K}_k (\mathbf{z}_k - \hat{\mathbf{z}}_k^-) \quad (17)$$

$$\mathbf{P}_k^+ = \mathbf{P}_k^- - \mathbf{K}_k \mathbf{P}_{vv} \mathbf{K}_k^T \quad (18)$$

where \mathbf{z}_k and \mathbf{R}_k are the measurement and its noise covariance, respectively; and \mathbf{K}_k is the Kalman gain matrix.

We summarize the implementation steps of the EKF and UKF in **Table 2**. Feedback of the biases can also be implemented to deal with the situation in which short-term correlated biases are superimposed on large long-term biases (See **Figure 1** for details on the data flow.)

Tests and Results

This section compares the performance of the EKF and the UKF using datasets collected in land vehicles with three different MEMS-based IMUs. The same set of GPS receivers and postprocessing software were used in all of the tests. We use several IMUs

	EKF	UKF
Gaussian random variables (GRV) propagation	Propagated analytically through the first-order linearization of the nonlinear system.	Represented using a minimal set of carefully chosen sample points (Sigma Points or SPs). The SP completely captures the true mean and covariance of the GRV, and when propagated through the true nonlinear system, captures the posterior mean and covariance accurately to the 2nd order (Taylor series expansion) for any nonlinearity.
Initialization	1. Initialize the error state and its covariance	1. Initialize the state and its covariance 2. Generate sigma points (SPs) for the initial states and covariance
Prediction	1. $\delta \hat{x}_{k+1}^- = \Phi_k \delta x_k^-$ 2. $P_{k+1}^- = \Phi_k P_k^- \Phi_k^T + Q_k$	1. Transform SPs through the INS mechanization 2. Compute mean and covariance from the transformed SPs 3. Generate sigma points for the predicted states and covariance
Update	1. $P_{vv} = H_k P_k^- H_k^T + R_k$ 2. $K_k = P_k^- H_k^T P_{vv}^{-1}$ 3. $\delta \hat{x}_k^+ = \delta \hat{x}_k^- + K_k (\delta z_k - H_k \delta \hat{x}_k^-)$ 4. $P_k^+ = (I - K_k H_k) P_k^- (I - K_k H_k)^T + K_k R_k K_k^T$	1. Transform SPs through the measurement model 2. Compute predicted measurement, \hat{z}_k^- , from the transformed SPs 3. Compute covariance between the state and the measurement, P_{xz} 4. Compute covariance of the innovation sequence, P_{vv} 5. $K_k = P_{xz} P_{vv}^{-1}$ 6. $\hat{x}_k^+ = \hat{x}_k^- + K_k (z_k - \hat{z}_k^-)$ 7. $P_k^+ = P_k^- - K_k P_{vv} K_k^T$ 8. Generate sigma points for the updated states and covariance
Feedback	Position, velocity, attitude and bias	Bias

TABLE 2. Implementation of the EKF and the UKF

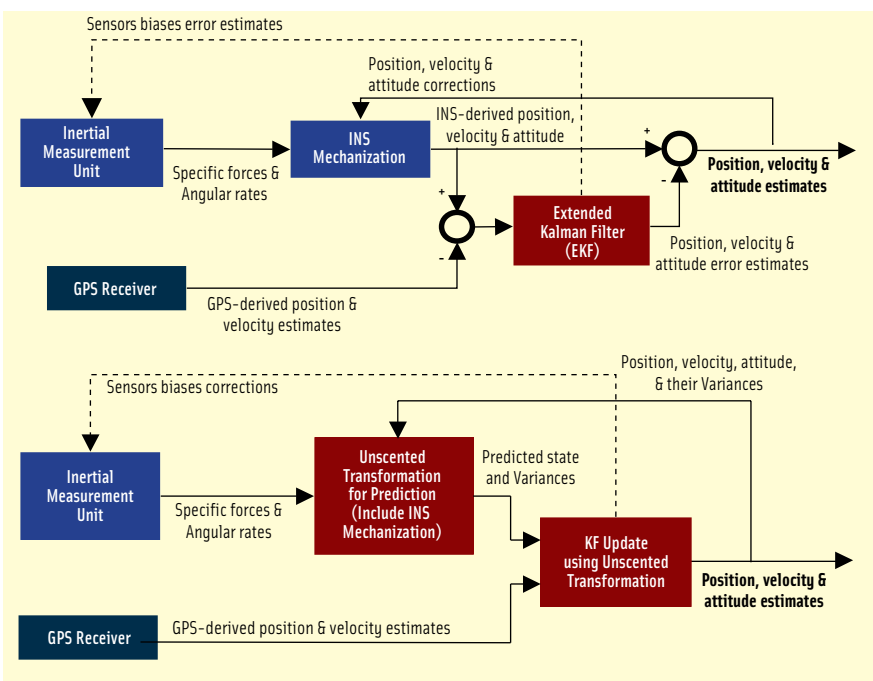


FIGURE 1 EKF Versus UKF Data Flow

surface-micromachining process and well calibrated including cross-axis misalignment and thermal drift compensation. The test was conducted by Applix Corporation in Toronto on March 5, 2003. The reference for the position, velocity and attitude are the smoothed best estimates (SBET) provided by Applix Corporation using postprocessing software and data from a tactical-grade IMU.

The attitude accuracy of the reference solution is known to be 0.02° for roll and pitch, and 0.05° for heading, when there are no GPS outages. The vehicle used in the test was a van, which was driven with both low dynamics (small loops) and typical high-way condition (large rectangular loops). For most of the time, horizontal and vertical position accuracies of the DGPS solution were about 2–3 centimeters and 4–9 centimeters, respectively.

In the second dataset, the IMU used quartz tuning-fork gyroscopes. The field test was conducted in the

in different field tests so as to be able to draw general conclusions about the two estimation algorithms. In this article, only the results of the custom-

built IMU sensor triads will be shown in detail as an example.

The first dataset used a prototype MEMS IMU manufactured through a

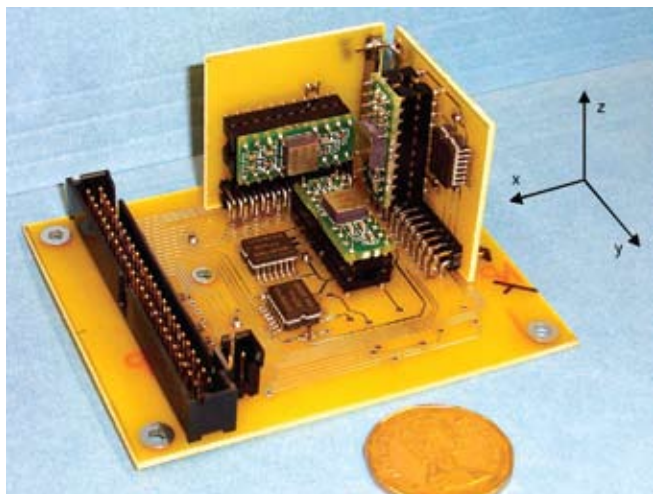


FIGURE 2 These sensor triads developed by the Mobile Multi-Sensor Systems Research Group, the University of Calgary (The dimension of the unit is 9.2x7.4x4.0 cm)

Research Park of the University of Calgary on March 4, 2003, operating a passenger vehicle and driven with relatively low speed in a small area. Because no other higher grade IMU was used, we used the smoothed solution from the unscented Kalman smoother (UKS) as the reference for this dataset.

The prototype MEMS IMU developed by the Mobile Multi-Sensor Systems Research Group at the University of Calgary and is shown in Figure 2. We refer to this IMU as the sensor triads. Since the original bias errors of the triad's sensors are as large as 20 deg/s for gyroscopes and 2 g for accelerom-

eters, we performed laboratory calibrations to obtain values for the biases, scale factors, and cross-axis misalignments. As a result, the biases of the gyroscopes and accelerometers have been reduced to 0.5 deg/s and 6 mg, respectively.

The third dataset was collected using the sensor triads mostly on a highway near the Calgary

International Airport in a joint test with NovAtel, Inc. using a test van. A smoothed DGPS/INS solution from a navigation-grade IMU served as the reference. Figures 3 and 4 show the trajectory and the accuracy of the DGPS solution, respectively. Although the sky was open for most of the time, buildings and bridges resulted in frequent GPS outages and significant DGPS solution degradation.

All three datasets were processed by the EKF and the UKF using parameters specifically tuned for each of the IMUs. Three processing scenarios for land vehicle navigations were considered to compare these two algorithms.

		EKF	UKF
Position (m)	North	0.081	0.080
	East	0.056	0.056
	Height	0.169	0.149
Attitude (deg)	Roll	0.230	0.252
	Pitch	0.366	0.346
	Heading	1.258	1.194

TABLE 3. Overall Performance (Sensor triads)

Scenario 1: Results with Continuous GPS Updates

The first scenario ran the algorithm with regular GPS updates. Our purpose was mainly to check whether the algorithms worked correctly or not. With continuous GPS measurements, the trajectory will generally follow that of the DGPS solution, while attitude errors will somehow reflect the quality of the integrated systems.

The results from the three MEMS systems show that the attitude accuracies can reach 0.1–0.4 degrees for pitch and roll, 0.7–1.3 degrees for heading. Table 3 lists the performance of the sensor triads as an example. For all three datasets, the EKF and the UKF showed similar performance.

Scenario 2: Results with Simulated GPS Outages

In the second scenario we processed the datasets with simulated GPS outages, which covered typical driving

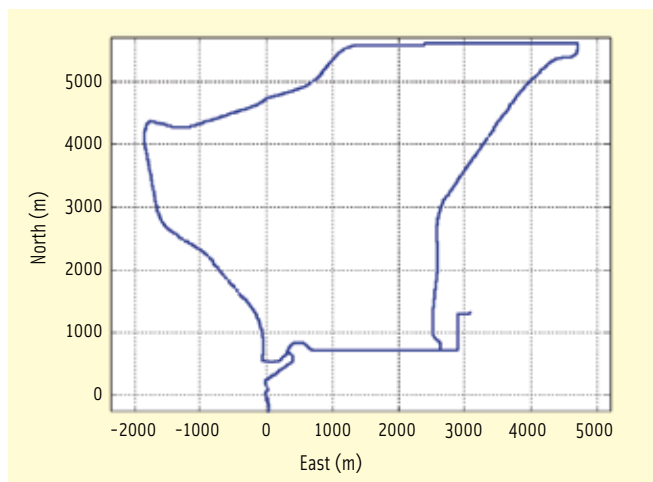


FIGURE 3 Trajectory of the third dataset

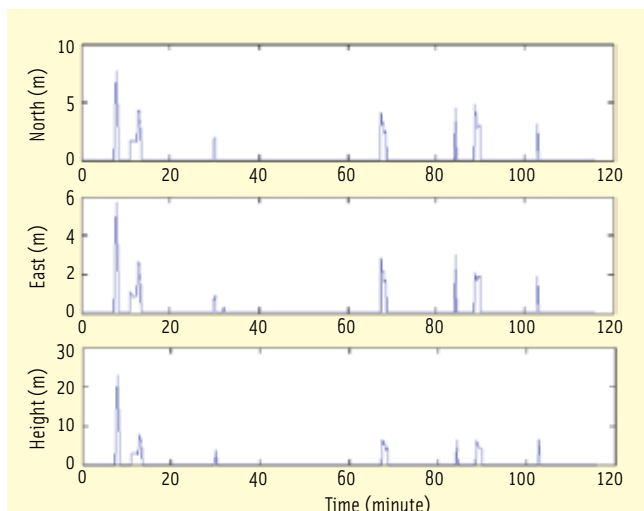


FIGURE 4 DGPS position accuracy of the third dataset

Outage	Direction	EKF	UKF
1	North (m)	58.203	57.731
	East (m)	46.653	47.066
	Height(m)	0.983	0.708
2	North (m)	17.086	17.452
	East (m)	11.873	11.802
	Height(m)	2.628	2.014
3	North (m)	0.813	0.422
	East (m)	28.424	29.180
	Height(m)	3.574	3.736
4	North (m)	22.054	22.093
	East (m)	5.200	5.002
	Height(m)	0.946	0.829
5	North (m)	11.583	11.858
	East (m)	1.402	0.773
	Height(m)	1.373	1.468
6	North (m)	15.656	15.297
	East (m)	15.020	14.708
	Height(m)	0.531	0.731

TABLE 4. Maximum errors during 30s GPS outages (ADI Sensor triads)

Time	Roll	Pitch	Heading
100–300 s	0.178	0.179	0.357
100–700 s	0.137	0.135	0.651

TABLE 5. RMS of the attitude errors for large initial attitude uncertainties (degrees)

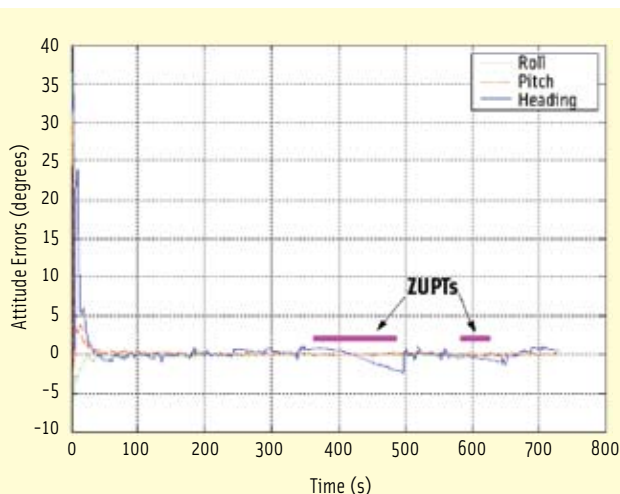


FIGURE 5 Attitude errors of the UKF under large initial attitude uncertainty (prototype IMU, first dataset).

conditions of land vehicles. It is a challenge for a low-cost INS to achieve high accuracy during GPS outages and also is a popular criterion for evaluating the performance of an integrated navigation system. Table 4 lists the maximum position errors during intentional 30-second GPS outages for the sensor triads. Again, the EKF and the UKF showed similar performance for each GPS outage in each direction. Generally, the average position drift after 30 seconds of GPS signal outages were from 10 to 30 meters for the tested MEMS IMUs.

Scenario 3: Results with Large Initial Attitude Errors

Typically, coarse alignment of an INS is done in stationary mode using leveling (by accelerometers) followed by gyro-compassing or, alternatively by using an analytical method that solves the gravity and the Earth rotation measurements in one step. For MEMS-based IMUs, however, the gyroscopes are not accurate enough to sense the Earth's rotation rate. Further, if the IMU is installed in a consumer vehicle, we cannot expect the user to wait until the alignment is finished. Hence, in-motion alignment is typically used.

The GPS-derived velocity can be used for coarse in-motion alignment if the vehicle's forward axis is parallel to the velocity vector. In airborne or shipborne applications, the vehicle may have lateral velocity components. In such cases, the initial heading derived from the GPS velocity can have large errors. Initial tilt errors may also be large if the vehicle is in high-dynamic motion.

All these issues will cause large initial attitude errors, which was our third scenario.

The test has been done by intentionally adding large initial attitude errors (30 degrees) for roll, pitch and heading. Under these serious initial conditions, the assumption of linear error behavior for the EKF could be violated.

Because the EKF described in this article used a standard computer frame error model, the EKF could not deal with large attitude errors and generated computational failure. On the other hand, the UKF converged as shown in Figure 5. The convergence has been made within 50 seconds, and the RMS of attitude errors after the convergence is listed in Table 5. For the EKF to cope with large attitude errors, a special INS error model must be developed. However, the UKF can deal with large attitude errors without devising a special model, and the transition from the large to small attitude errors is seamless.

Conclusions

This article has reviewed the implementation of the EKF and the UKF and compared their performance for integrated low-cost inertial navigation systems. Both the EKF and the UKF work well for the integration of typical MEMS-based IMU and GPS. Performance of the EKF and the UKF is generally similar (in both cases when GPS signals are available and when GPS signals are blocked).

The EKF requires a special navigator error model to handle large initial attitude errors. However, the UKF can deal with such errors without additional effort, and the transition from the large to small attitude uncertainties is seamless. Therefore, the UKF will be beneficial in the applications where in-motion alignment is required.

Acknowledgements

This study was funded by research grants from Natural Science and Engineering Research Council of Canada (NSERC) and Geomatics for Informed Decisions (GEOIDE), Network Centers of Excellence (NCE) awarded to Dr. Naser El-Sheimy. The authors would like to thank Dr. Bruno M. Scherzing-

er, Applanix Corporation, for providing a dataset for the ISIS IMU test.

Manufacturers

OEM4 and MiLlennium from NovAtel Inc., Calgary, Alberta, Canada, were used in the tests. The post-processed DGPS position solutions from GrafNav software from Waypoint Consulting, Inc., Calgary, were used as the measurement updates for the EKF and UKF in all datasets. The custom-built IMU integrates three accelerometers (ADX105) and three gyroscopes (ADXRS150), both from Analog Devices Inc., Norwood, Massachusetts, USA. The first dataset used a prototype IMU (ISIS IMU) made by Inertial Science, Inc., Newbury Park, California, USA. The ISIS IMU used MEMS gyroscopes from Analog Devices, Inc. The reference for the position, velocity and attitude are the smoothed best estimates (SBET) using POSPac software from Applanix Corporation (a Trimble company), Richmond Hill, Ontario, Canada. To process the data using a tactical-grade IMU the LN-200 from Northrop Grumman, Navigation Systems Division, Woodland Hills, California. The second dataset used a MotionPak II IMU from BEI Systron Donner, Inertial Division, Concord, California. The third dataset was collected using the sensor triads and The smoothed DGPS/INS solution from a navigation-grade C-IMU, Honeywell Inc., Phoenix, Arizona, USA. All the three data were processed using AINS (Aided Inertial Navigation System (AINS™) software developed by the Mobile Multi-Sensor Systems Research Group at the University of Calgary.

Additional Resources

BEI Technologies, Inc. (2002). MotionPak® II Operating Manual. Systron Donner Inertial Division, BEI Technologies, Inc.

Benson Jr., D. O. (1975). A Comparison of Two Approaches to Pure-Inertial and Doppler-Inertial Error Analysis. *IEEE Transactions on Aerospace and Electronic Systems*, AES-11(4):447–455

Britting, K. R. (1971). *Inertial Navigation Systems Analysis*. John Wiley & Sons, Inc.

Brown, R. G. and Hwang, P. Y. C. (1992). *Introduction to Random Signals and Applied Kalman Filtering*. John Wiley & Sons, Inc., second edition

El-Sheimy, N. and Niu, X. (2004). The Development of Low-Cost MEMS-Based IMU for Land Vehicle Navigation Applications. Presentation in GEOIDE Annual Meeting, Gatineau, Québec, Canada (CD)

Farrell, J. A. and Barth, M. (1998). *The Global Positioning System & Inertial Navigation*. McGraw-Hill

Hou, H. and El-Sheimy, N. (2003). Inertial Sensors Errors Modeling Using Allan Variance. In *Proceedings of ION GPS/GNSS*, pages 2860–2867, Portland, Oregon

Julier, S. J. (2003). The Spherical Simplex Unscented Transformation. In *Proceedings of the IEEE American Control Conference*, pages 2430–2434, Denver, Colorado

Julier, S. J. and Uhlmann, J. K. (1996). A General Method for Approximating Nonlinear Transformations of Probability Distributions. Technical report, Department of Engineering Science, University of Oxford, Oxford, OX1 3PJ, UK

Julier, S. J. and Uhlmann, J. K. (2002). The Scaled Unscented Transformation. In *Proceedings of the IEEE American Control Conference*, pages 4555–4559, Anchorage AK, USA

Rogers, R. M. (1997). IMU In-Motion Alignment Without Benefit of Attitude Initialization. *Navigation: Journal of The Institute of Navigation*, 44(3):301–311

Scherzinger, B. M. (1996). Inertial Navigator Error Models for Large Heading Uncertainty. In *IEEE Position Location and Navigation Symposium*, pages 477–484

Scherzinger, B. M. and Reid, D. B. (1994). Modified Strapdown Inertial Navigator Error Models. In *IEEE Position Location and Navigation Symposium*, pages 426–430, Las Vegas, Nevada

Schwarz, K.-P. and Wei, M. (2000). INS/GPS Integration for Geodetic Applications. Lecture Notes ENGO623. Dept. of Geomatics Eng., The University of Calgary, Calgary, Canada

Shin, E.-H. (2001). Accuracy Improvement of Low Cost INS/GPS for Land Applications. UCGE Reports Number 20156, The University of Calgary, Calgary, Alberta, Canada

Shin, E.-H. (2004). A Quaternion-Based Unscented Kalman Filter for the Integration of GPS and MEMS INS. In *Proceedings of ION GPS/GNSS*, pages 1060–1068, Long Beach, California, USA

Shin, E.-H. and El-Sheimy, N. (2004). An Unscented Kalman Filter for In-Motion Alignment of Low-Cost IMUs. In *Proceedings of IEEE Position, Location, and Navigation Symposium*, pages 273–279, Monterey, CA.

Wan, E. A. and van der Merwe, R. (2001). Kalman Filtering and Neural Networks, Haykin, S. (Ed.), chapter 7. John Wiley & Sons, New York

Authors

Naser El-Sheimy is a professor and the leader of the Mobile Multi-sensor Research Group at the University of Calgary, Canada. He holds a Canada Research Chair (CRC) in Mobile Multi-Sensors Geomatics Systems. El-Sheimy's area of expertise is in the integration of GPS/INS/imaging sensors for mapping and GIS applications with special emphasis on the use of multi-sensors in mobile mapping systems. He achieved a B.Sc. (Honor) degree in civil engineering and an M.Sc. Degree in surveying engineering from Ain Shams University, Egypt, and a Ph.D. in geomatics engineering from the University of Calgary, Alberta, Canada. Currently, El-Sheimy is the chair of the International Society for Photogrammetry and Remote Sensing Working Group on "Integrated Mobile Mapping Systems," the vice-chair of the special study group for mobile multi-sensor systems of the International Association of Geodesy and the chairman of the International Federation of Surveyors (FIG) working group C5.3 on Integrated Positioning, Navigation and Mapping Systems.

Eun-Hwan Shin is currently a navigation analyst for Applanix Corporation, in Toronto, Canada. He obtained his Ph.D. from the Department of Geomatics Engineering at the University of Calgary. He holds a B.Sc. and an M.Sc. from the Seoul National University in Korea and an M.Sc. in geomatics engineering from the University of Calgary. Shin has developed a MatLab INS toolbox during his Ph.D. program at U of C. His research interest is on developing estimation methods for low-cost inertial navigation systems.

Xiaoji Niu is a postdoctoral fellow and a member of the mobile multi-sensor research group in the Department of Geomatics Engineering at the University of Calgary. He has a Ph.D. in the Department of Precision Instruments & Mechanology at Tsinghua University. Niu received the B.S. degrees (with honors) in both mechanical engineering and electrical engineering from Tsinghua University in 1997. His research interest focuses on the low-cost GPS/INS integration technologies and micromachined (that is, MEMS) inertial sensors and systems. 